Advances in Materials Technology for Fossil Power Plants
Proceedings from the Seventh International Conference
October 22–25, 2013, Waikoloa, Hawaii, USA
https://doi.org/10.31399/asm.cp.am-epri-2013p0459

D. Gandy, J. Shingledecker, editors

SIMILAR AND DISSIMILAR WELDING OF NICKEL-BASED SUPERALLOYS FOR A-USC STEAM TURBINE ROTORS IN NEXTGENPOWER PROJECT

Stanislav Hreben, Petr Vitek, Vaclav Zednik, Lubos Prchlik
DOOSAN SKODA POWER, Ltd., Tylova 1/57, Plzen, 31600, Czech Republic

ABSTRACT

Carbon Capture and Storage (CCS) has become promising technology to reduce CO_2 emissions. However, as a consequence of CCS installation, the electrical efficiency of coal fired power plant will drop down. This phenomenon requires increase in base efficiency of contemporary power plants. Efficiency of recent generation of power plants is limited mainly by maximum live steam temperature of 620°C. This limitation is driven by maximal allowed working temperatures of modern 9–12% Cr martensitic steels. Live steam temperatures of 750°C are needed to compensate the efficiency loss caused by CCS and achieve a net efficiency of 45%. Increase in the steam temperature up to 750°C requires application of new advanced materials. Precipitation hardened nickel-based superalloys with high creep-rupture strength at elevated temperatures are promising candidates for new generation of steam turbines operating at temperatures up to 750°C. Capability to manufacture full-scale forged rotors and cast turbine casings from nickel-based alloys with sufficient creep-rupture strength at 750°C/10^5 hours is investigated. Welding of nickel-based alloys in homogeneous or heterogeneous combination with 10% Cr martensitic steel applicable for IP turbine rotors is showed in this paper. Structure and mechanical properties of prepared homogeneous and heterogeneous weld joints are presented.

INTRODUCTION

Reduction of CO_2 emissions is one of the main goals of EU in the next years. Particularly, 20% reduction will be required by EC in 2020. To reduce CO_2 emissions to above mentioned level implementation of Carbon Capture and Storage (CCS) in coal power plants is needed. However, application of CCS technology is related with decrease of power plant efficiency. To compensate this decrease in efficiency, higher temperatures of live steam flowing through turbine are needed. Of course, higher steam temperature has significant impact on material selection for boiler and turbine components. Live steam temperatures of 700 – 750°C call for application of nickel-based superalloys with sufficiently high creep rupture strength at 750°C/10^5h [1, 2]. NEXTGENPOWER is unique international collaborative project demonstrating application of new alloys and coatings in boiler, turbine and interconnecting pipework and should show new directions in design of A-USC power plant. In this project, precipitation hardened gamma-prime nickel-based alloy Nimonic 263 (A263) was selected as a promising material for high pressure (HP) steam turbine rotor. In the case of intermediate pressure (IP) steam turbine rotors, it is really demanded to master dissimilar weld joint of nickel-based alloys with advanced 9-12% Cr martensitic steels in order to manufacture welded IP rotor. Based on the heat balance calculations of NEXTGENPOWER A-USC power plant, inlet steam temperature of IP turbine is 750°C. However, IP turbine outlet stem temperature is around 350°C. Thus, it is not necessary to manufacture whole IP turbine rotor from A263 as a single piece, but combine this material with less expensive 9-12% Cr martensitic steels that can be applied in less hot section of IP turbine, see

Fig. 2. This will significantly reduce the price of turbine set. Manufacture of welded rotors combining 12% Cr and low alloy martensitic steels has been developed and demonstrated [3-4]. With respect to A263, similar weld joint has been mastered in past [5]. Recommended approach is to weld this material in solution treated condition. As a filler metal, Nimonic 263 is typically used. However, precipitation hardening 800°C/8hours should be carried out after welding in order to achieve sufficiently high strength and creep resistance of both base material and filler metal. This approach cannot be used for dissimilar weld joint of A263 with 9-12% Cr martensitic steel because of tempering temperatures of 9-12% Cr steel. Particularly, COST F (X14CrMoVNbN10-1) martensitic steel with tempering temperatures around 700°C was chosen as a rotor material for less hot section of the IP turbine in this project because of its very good creep properties at temperatures up to 600°C.

Figure 1: Dissimilar weld joint Nimonic 263 + COST F applicable for IP turbine of A-USC power plant.

With respect to above mentioned aspects, A263 has to be welded in precipitation hardened condition (800°C/8h) in the case of dissimilar weld joint A263 + COST F, because precipitation hardening cannot be carried out after welding due to tempering temperatures (~700°C) of COST F steel on the other side of the weld joint. Post-weld heat treatment (PWHT) overcoming tempering temperature of COST F would negatively affect strength and creep properties of this material. Dissimilar welding process for above mentioned material combination A263 + COST F is described and studied in this paper. TIG hot wire narrow gap welding was used to demonstrate manufacture of welded rotors. Optimal PWHT was found with respect to the best combination of strength and toughness given by rotor design point of view. Mechanical properties of similar (A263 + A263) and dissimilar (A263 + COST F) are analyzed and discussed in this paper.

EXPERIMENTAL

All discussed similar and dissimilar weld joints were processed by TIG hot wire narrow gap welding. Unique experimental welding stand allowing welding of rotor parts in vertical position was used. Welding head was kept in fixed position whereas the welded samples rotated on the table. Example of the welded samples in vertical configuration on the table of the experimental welding stand is shown on Fig. 2. Nickel-based welding consumable not requiring post-welding precipitation hardening was used. Two different welding torches V2 and WP27 were applied for root and filling passes, respectively. Samples with diameter of 160 mm and welding depth 50 mm were used for similar combination A263 + A263. In the case of dissimilar weld joint A263 + COST F, discs with diameter of 300 mm and welding depth 100 mm were used. Table 1 shows material composition of base materials used. In the case of similar weld joint A263 + A263, no pre-heating was applied on welded samples. The interpass temperature was kept below 100°C in order to avoid hot cracking. Welding parameters found for similar combination were used as a background for welding of heterogeneous combination A263 + COST F. In the case of dissimilar combination, two approaches, with and without cladding of COST F with nickel-based cladding metal, were applied. Pre-heating of COST F was used during welding process without cladded

COST F. In the case of option with cladded COST F, pre-heating of COST F discs was used during cladding process. However, no pre-heating of cladded COST F was applied during dissimilar welding A263 + COST F. For both variants with/without cladded COST F, interpass temperature was kept again below 100°C during narrow gap welding of A263 + COST F.

Figure 2: Configuration of welding samples Nimonic 263 + Nimonic 263 Ø160mm on experimental welding stand with narrow gap torch.

PWHT of welded samples was carried out in electric furnace with various temperatures and durations. Macrostructure and microstructure evaluation, tensile, hot tensile test and Charpy impact test were carried out for all similar weld joints treated with different PWHTs and both variants of dissimilar weld joint (with/without cladded COST F). Tensile test values were calculated as an average of three measured samples. Impact energies values were calculated as an average of two or three tested samples, depending on available amount of test material.

		C	Si	Mn	S	Ni	Cr	Mo	Al	Co	Cu	Ti
Ø160 mm	**A 263**	0.051	0.024	0.02	0.00051	52.0	19.59	5.77	0.422	19.89	<0.01	2.21

		C	Si	Mn	S	Ni	Cr	Mo	Al	Co	Cu	Ti
Ø300 mm	**A 263**	0.041	0.109	0.16	0.001	53.0	19.2	5.7	0.51	19.3	0.008	2.27

		C	Si	Mn	S	Ni	Cr	Mo	Al	V	Nb	N
Ø300 mm	**COST F**	0.13	0.08	0.54	0.001	0.57	10.42	1.50	0.009	0.17	0.05	0.057

Table 1: Chemical composition of base materials.

RESULTS AND DISCUSSION

Similar Weld Joint A263 + A263

Properties of similar weld joint A263 + A263 has been investigated at first as a background for final dissimilar weld joint A263 + COST F. A263 was welded in precipitation hardened condition. Three different PWHT were applied and compared with not heat treated weld joint. All three PWHTs were carried out with the same temperature but different duration, where time_1<time_2<time_3. Temperature of PWHT was chosen with respect to operation temperature

of the weld joint in turbine and typical tempering temperatures of COST F steel used in dissimilar combination of A263 + COST F. Results on tensile test at 20°C are shown in Fig. 3. Cap, filler and root of the weld joint were analyzed. All the samples were broken in the filler metal. As can be seen in Fig. 3, longer PWHT leads to increase of tensile strength. This phenomenon is most likely attributed to carbide formation and precipitation of gamma prime phase in filler metal. Results on Charpy impact tests are shown in Fig. 4 for various PWHTs. V-notch was placed in filler metal and heat affected zone (HAZ) for cap and root of the weld joint. As expected, decrease in impact energy is related with growing tensile strength of weld joint. Longer PWHT time leads to more strength but less ductile structure of filler metal and HAZ.

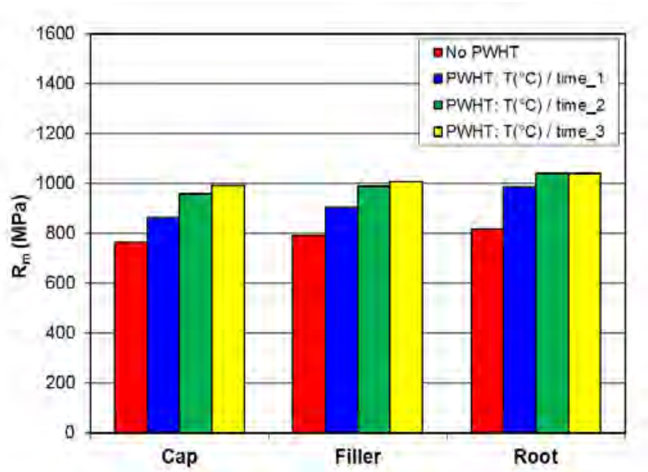

Figure 3: Room temperature tensile strength of weld joint A263 + A263 measured for various PWHTs. Tensile properties were measured in cap, filler and root area of the weld joints.

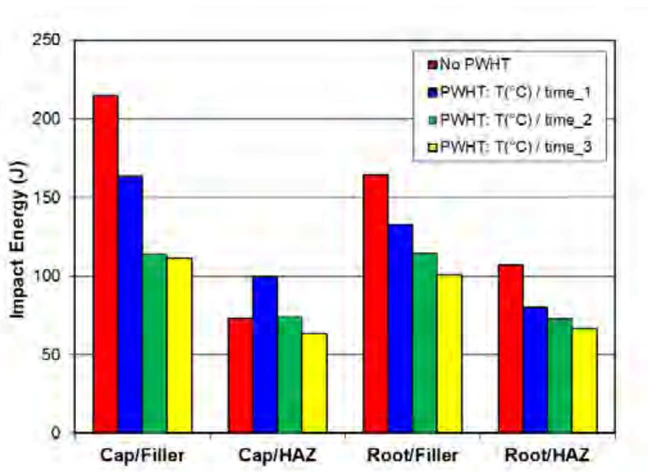

Figure 4: Charpy impact test performed at 20°C of weld joint A263 + A263 treated with various PWHTs. Impact energy was measured for filler metal and HAZ in root and cap area of the weld joint.

From rotor design perspective, optimal combination of the strength and toughness is required. Thus, PWHT T(°C)/time_2 was chosen as the best option optimizing tensile and fracture toughness properties of filler metal and HAZ between A263 and filler metal. T(°C)/time_2 PWHT was selected as a default heat treatment for dissimilar combination A263 + COST F. For optimal PWHT T(°C)/time_2, hot tensile test at 700 and 750°C was carried out and compared to results measured at room temperature, see Fig. 5. Cap, filler and root of the weld joint were analyzed. Elevated temperatures of tensile test led to decrease of tensile strength from 1000 MPa to 700 MPa. All the samples were broken in filler metal.

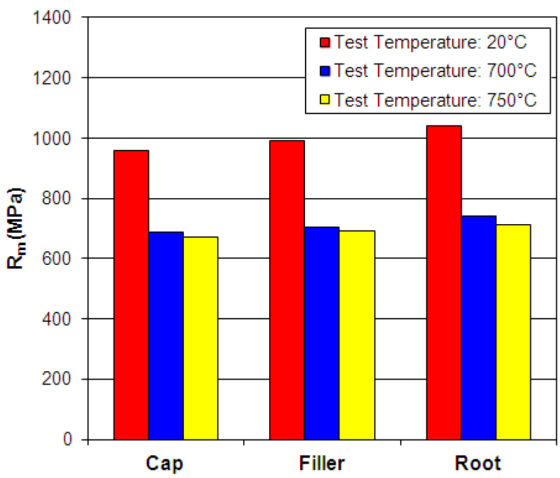

Figure 5: Tensile strength at elevated temperatures measured for similar weld joint A263 + A263 treated with optimal PWHT T(°C)/time_2. Tensile properties were analyzed for cap, filler and root area of the weld joints.

Dissimilar Weld Joint A263 + COST F

To demonstrate dissimilar welding of A263 + COST F, welding parameters found for similar combination A263 + A263 were used. As has been indicated, two approaches were applied to master dissimilar welding of A263 + COST F. In the first case, easier approach was chosen and COST F steel was welded without nickel-based cladding. Material A263 was used in precipitation hardened condition. In this case, it was necessary to pre-heat COST F prior and during welding process. Applied pre-heating caused difficulties in keeping of interpass temperatures below recommended 100°C, which increases risk of hot cracking. In the second case, pre-heated COST F was cladded with nickel-based cladding metal at first. After cladding process, residual stress relief heat treatment was carried out. Then, the nickel-based cladding of COST F was machined down to required shape of the bevel. Welding of A263 and cladded COST F was performed without preheating of cladded COST F counter piece. This approach enables to keep interpass temperatures as low as possible. For both variants, with/without cladding of COST F, optimal PWHT found for similar weld joint A263 + A263 was used to relief the internal stresses. Results of room temperature tensile test are shown on Fig. 6 for both variants with/without cladding of COST F. All the samples were broken in COST F base material, which indicates that tensile strength of filler metal is higher than tensile strength of COST F base material. In previous paragraph dealing with similar weld joint A263 + A263, all the samples were broken in filler metal. For PWHT T(°C)/time_2, tensile strength R_m and yield strength $R_{p0.2}$ of similar weld joint

A263 + A263 ranged in 950 – 1050 MPa, which is significantly higher value than certified tensile strength R_m = 870 MPa of COST F base material used for dissimilar welding tests. These findings point out that COST F is the weakest material in dissimilar weld joint from the tensile strength point of view. As mentioned, certified tensile and yield strength of COST F base material are R_m = 870 MPa and $R_{p0.2}$ = 730 MPa, respectively. However, tensile test of both variants of weld joints showed that tensile and yield strength of COST F after welding operation and application of PWHT are lower than those of the same material prior welding, see R_m = 750 – 800 MPa and $R_{p0.2}$ = 600 – 650 MPa after welding and PWHT in Fig. 6.

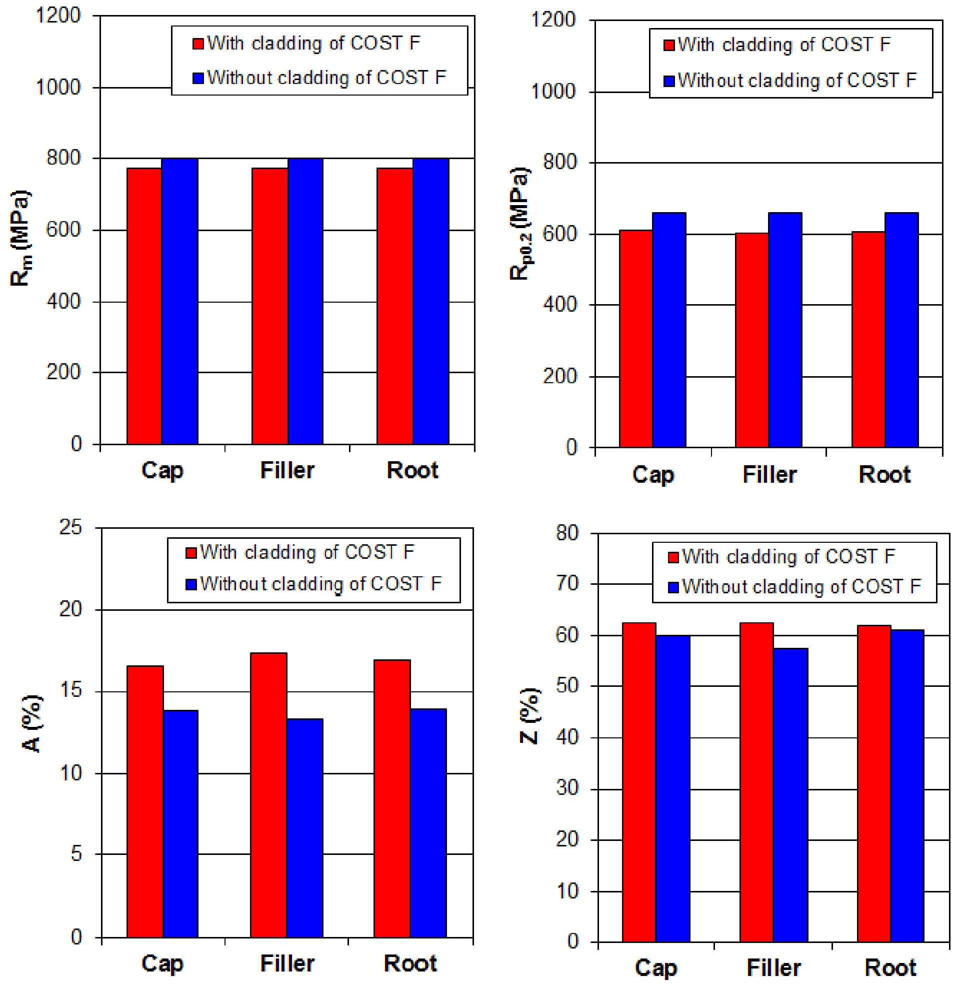

Figure 6: Tensile test results of dissimilar weld joint A263 + COST F carried out at room temperature for both variants with/without cladding of COST F.

This decrease of tensile and yield strength of COST F after welding is most likely related with PWHT of weld joint at temperatures very close to tempering temperature of COST F base material. Moreover, approach with cladding of COST F provides slightly lower tensile and yield strength then approach without cladding. This can be explained by longer exposition of COST F base material during PWHT to temperatures close to tempering temperature of COST F for variant with cladding of COST F. Particularly, two PWHTs, one for cladding and one for whole weld joint, were applied. On the other hand, only one PWHT was used for variant without cladding of COST F. Elongation A(%) and reduction in area Z(%) have opposite manner than tensile strength. For variant with cladding of COST F, A(%) and Z(%) are higher than for variant without cladding. From perspective of tensile properties and complexity of weld joint manufacture, variant without cladding of COST F is simpler and provides higher tensile strength at still sufficiently high elongation.

Results on Charpy impact test are shown on Fig. 7. V-notch was placed in various areas of the weld joints. Particularly, HAZ between COST F and cladding, cladding, HAZ between cladding and filler metal, filler metal, HAZ between filler metal and A263 were analyzed for cap and root of the weld joint for option with cladding of COST F. For variant without cladding on COST F, HAZ between COST F and filler metal, filler metal, HAZ between filler metal and A263 were analyzed for cap and root of the weld joint.

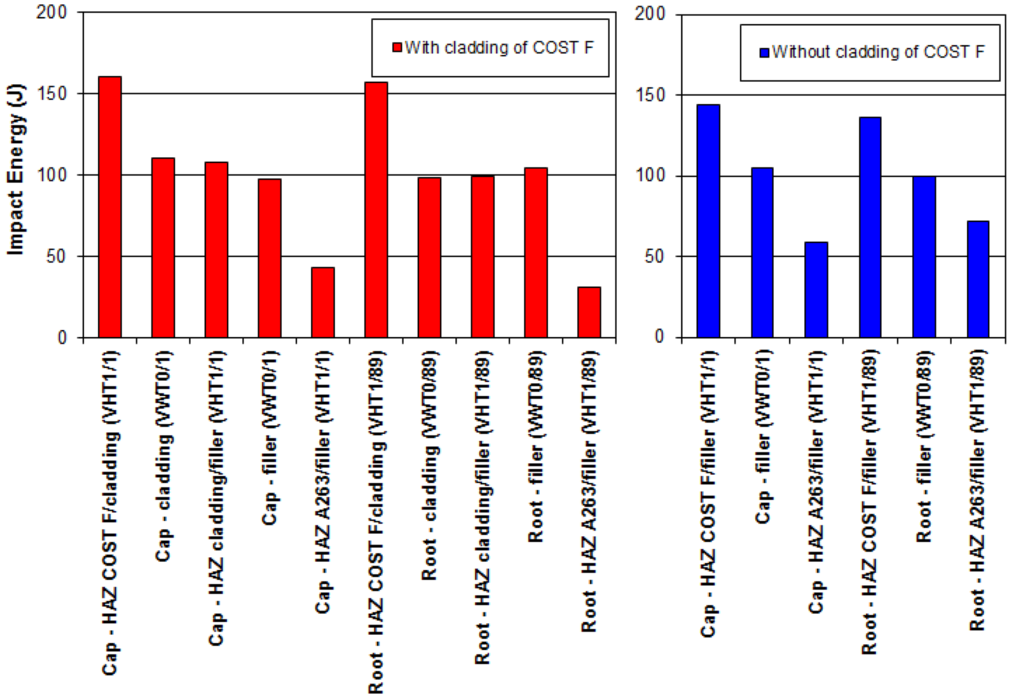

Figure 7: Charpy impact test of dissimilar weld joint A263 + COST F carried out at room temperature for both variants with/without cladding of COST.

As can be seen on Fig. 7, most critical area of the weld joint is HAZ between filler metal and A263 (see the lowest impact energies measured in this location for both variants with/without cladding of COST F). This phenomenon is most likely related with microstructure changes of A263 due to welding process. To confirm this theory, further and more detail investigation of microstructure especially in this transition zone would be needed. However, from the perspective of rotor design and structural calculations, even the lowest measured impact energies are sufficiently high and acceptable.

Macrostructure of dissimilar weld joint A263 + COST with/without cladding of COST F is shown on Fig. 8. Cross-sections taken from three different locations were analyzed for both variants. No defects and cracks were indicated on all analyzed cross-sections. Both weld joints met requirements of quality degree B (the highest quality) given by EN ISO 5817.

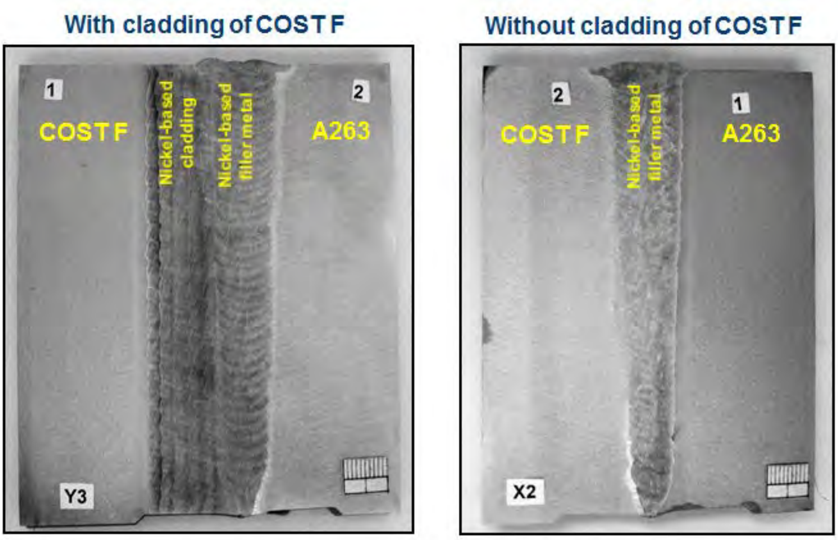

Figure 8: Macrostructure of dissimilar weld joint A263 + COST F taken for both variants with/without cladding of COST F.

Next step in NEXTGENPOWER project in terms of dissimilar rotor welding is demonstration of full-scale rotor welding on production welding stand in Doosan Skoda Power. Based on achieved experiences, dissimilar full-scale weld joint A263 + COST F with diameter of 1000 mm will be welded and extensively tested.

CONCLUSIONS

It was demonstrated that Nimonic 263 can be successfully welded in precipitation hardened condition. Optimal PWHT was found for similar weld joint A263 + A263 with respect to optimal combination of tensile strength and toughness. Dissimilar welding of A263 + COST F was demonstrated. Two approaches with/without cladding of COST F with nickel-based cladding metal were investigated. With respect to tensile strength, toughness and severity of welding process, variant without cladding of COST F seems to be more effective approach for this material combination. Macrostructure of both dissimilar weld joints A263 + COST F with/without cladding of COST F met requirements on the highest quality degree given by EN ISO 5817.

ACKNOWLEDGEMENTS

The authors would like to acknowledge the support of NEXTGENPOWER project (Project no: ENER/FP7EN/249745/”NEXTGENPOWER”) and to the European Commission for financial support.

REFERENCES

[1] N. Lückemeyer, H. Kirchner, H. Almstedt, “Challenges in advanced-USC steam turbine design for 1300°F/700°C”, *Proceedings of ASME Turbo Expo 2012*, Copenhagen, Denmark, June 2012.

[2] M. Fukuda, E. Saito, Y. Tanaka, T. Takahashi, S. Nakamura, J. Iwasaki, S. Takano, S. Izumi, “Advanced USC technology development in Japan”, *Proceedings of Advances in Materials Technology for Fossil Power Plants 2010*, Santa Fe, New Mexico, USA, August 2010.

[3] T. Shige, S. Itou, R. Magoshi, T. Ichimura, Y. Kondou, “Development of Large-Capacity, Highly Efficient Welded Rotor for Steam Turbines“, *Mitsubishi Heavy Industry Ltd. Technical review*, Vol. 38, No. 1 (2001).

[4] J. Hutchinson, R. Conroy, R. Stalker, “Fabricated Turbine Rotors for Advanced Steam Turbines“, *Siemens Power Generation*, *Public Report*, August 2004.

[5] J. Minwoo, L. Jae-Hyun, W. T. Kwan, K. Sangshik, “Effect of Welding and Post-weld Heat Treatment on Tensile Properties of Nimonic 263 at Room and Elevated Temperatures”, *Metallurgical and Materials Transactions A*,Vol. 42, No. 4 (2011), pp. 974-985.